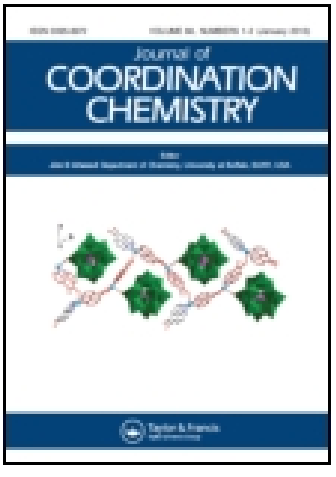

Journal of Coordination Chemistry
Publication details, including instructions for authors and subscription information:
http://www.tandfonline.com/loi/gcoo20

Synthesis, characterization, structural investigation, and antimicrobial studies of mononuclear Zn(II), Cd(II), and Ag(I) complexes of an N_3O Schiff base

Pankaj K. Pal[a], Ananya Banerjee[a], Ranjan Bhadra[a], Atish D. Jana[b] & Goutam K. Patra[ac]

[a] Department of Chemistry and R&D Section, Vijoygarh Jyotish Ray College, Kolkata, India

[b] Department of Physics, Behala College, Kolkata, India

[c] Department of Chemistry, Guru Ghasidas Vishwavidyalaya, Bilaspur, India

Accepted author version posted online: 04 Aug 2014.Published online: 09 Sep 2014.

To cite this article: Pankaj K. Pal, Ananya Banerjee, Ranjan Bhadra, Atish D. Jana & Goutam K. Patra (2014) Synthesis, characterization, structural investigation, and antimicrobial studies of mononuclear Zn(II), Cd(II), and Ag(I) complexes of an N_3O Schiff base, Journal of Coordination Chemistry, 67:18, 3107-3120, DOI: 10.1080/00958972.2014.951346

To link to this article: http://dx.doi.org/10.1080/00958972.2014.951346

Journal of Coordination Chemistry, 2014
Vol. 67, No. 18, 3107–3120, http://dx.doi.org/10.1080/00958972.2014.951346

Synthesis, characterization, structural investigation, and antimicrobial studies of mononuclear Zn(II), Cd(II), and Ag(I) complexes of an N_3O Schiff base

PANKAJ K. PAL†, ANANYA BANERJEE†, RANJAN BHADRA†, ATISH D. JANA‡ and GOUTAM K. PATRA*†§

†Department of Chemistry and R&D Section, Vijoygarh Jyotish Ray College, Kolkata, India
‡Department of Physics, Behala College, Kolkata, India
§Department of Chemistry, Guru Ghasidas Vishwavidyalaya, Bilaspur, India

(*Received 16 January 2014; accepted 21 July 2014*)

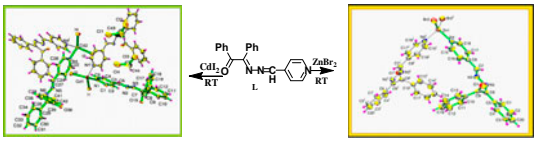

A Zn(II), Cd(II) and Ag(I) mononuclear complexes of an N_3O Schiff base have been synthesized. The crystal structures of these complexes have been determined. The complexes have antibacterial activity against the bacteria *K. pneumoniae 114*, *E. coli K88*, *S. typhi ATCC 34*, *B. subtilis UC564,* and *S. aureus ATCC25923* and antifungal activity against *A. niger*, *A. oryzae*, *P. notatum,* and *S. cerevisiae*.

An N_3O Schiff base (**L**), 1 : 1 condensate of benzil monohydrazone and 4-pyridine carboxaldehyde, and its Zn(II), Cd(II), and Ag(I) complexes were synthesized and characterized by elemental analyses and various spectroscopic techniques. The crystal structures of $[ZnL_2Br_2]$ (**1**), $[CdL_2I_2]\cdot CH_2Cl_2$, (**2**)$\cdot\mathbf{CH_2Cl_2}$, and $[Ag(L)_2]ClO_4$ (**3**) have been determined using X-ray crystallography. The Zn(II) and Cd(II) complexes show a tetrahedral configuration whereas in the asymmetric unit of **3**, two independent coordination units of Ag(I) are present. Carbonyl–silver interaction, weak C–H···O interaction, and also π–π interaction are present in **3** in the solid state. The synthesized complexes have antibacterial activity against *Klebsiella pneumoniae 114*, *Escherichia coli K88*, *Salmonella typhi ATCC 34*, *Bacillus subtilis UC564,* and *Staphylococcus aureus ATCC25923*. The results showed that in some cases the antibacterial activities of the complexes were comparable to standard antibiotics Tetracycline and Streptomycin. The antifungal activities of the complexes were also studied for *Aspergillus niger*, *Aspergillus oryzae*, *Penicillium notatum,* and *Saccharomyces cerevisiae*. MIC values of **1**, **2**$\cdot\mathbf{CH_2Cl_2}$, and **3** are less than the Nystatin standard.

Keywords: NNNO-donor ligands; Mononuclear Zn(II), Cd(II), and Ag(I) complexes; Antimicrobial activity; Antifungal activity; Crystal structure

*Corresponding author. Email: patra29in@yahoo.co.in

1. Introduction

Schiff bases are chelating ligands in coordination chemistry and their metal complexes are widely studied [1–4] for their biochemical, analytical, antimicrobial, antifungal, antitumor, therapeutic, herbicidal, and industrial applications [5–12]. Schiff base ligands containing N,O donor sites possess many advantages, such as easy synthesis, readily adjusted subsidiary ligands, tunable steric and electronic coordination environments on the metal center, and the ability to show interesting properties by their metal complexes [13, 14]. Metal complexes of these types of ligands show versatile molecular frameworks [15], interesting solvatochromic and nanomolecular properties [16, 17], and exciting biological activity [18].

Complexes of d^{10} metal ions such as zinc(II), cadmium(II), and silver(I) are of interest because these metals are involved in many biological molecules [19]. Zinc-containing compounds are useful model compounds for biochemical research, as zinc(II) plays an important role in several zinc-containing metal enzymes such as zinc peptidases [20], human carbonic anhydrase [21], and alkaline phosphatase [22]. Though Cd(II) is a toxic metal [23], complexes have potential applications in catalysis [24], optical properties evolution [25], clathration [26], the vulcanization of diene rubbers [27], and in the treatment of hyperthyroidism [28]. Ag(I) ions are more attuned with biological system [29], with complexes exhibiting diverse coordination geometries as well as antimicrobial, antifungal, and anticancer activities [30–32].

As part of our ongoing research to study a series of supramolecular complexes of iminopyridyl Schiff base ligands and d^{10} metal ions as building blocks, we describe here the synthesis, structure, and biological activity of an N_3O donor Schiff base, **L** (a 1 : 1 condensate of benzil monohydrazone and 4-pyridine carboxaldehyde) and its Zn(II), Cd(II), and Ag(I) complexes, **1**, **2**, and **3**, respectively.

2. Experimental

2.1. *Materials and methods*

Benzil monohydrazone was synthesized by a reported procedure [33]. All other reagents were procured commercially and used without purification. Microanalyses were carried out using a Perkin-Elmer 2400II elemental analyzer. Infrared (IR) spectra and solution electronic spectra were recorded on Nicolet Magna-IR (Series II) and Shimadzu UV-160A spectrophotometers, respectively. ^{1}H NMR and electrospray ionization mass (ESI-MS) measurements were made using a Bruker Avance 400 MHz spectrometer and Finnigan LCQ Decaxp MAX mass spectrometer, respectively.

2.2. *Synthesis of L*

Benzil monohydrazone (1.87 g, 7.86 mM) was dissolved in 30 mL of anhydrous methanol. To this colorless solution, 0.75 mL (7.86 mM) of freshly distilled 4-pyridine carboxaldehyde was added. The resulting yellow mixture was refluxed for 8 h, maintaining dry atmosphere. Then it was slowly cooled to room temperature to yield yellowish crystalline solid. After that the solid was filtered off and dried in air. Crystals suitable for X-ray analysis were obtained by slow evaporation of *n*-hexane solution. Yield, 1.85 g (75%). M.p.: 128 °C. ^{1}H NMR (200 MHz) (δ, ppm) 8.60 (d, 2H), 8.52 (s, 1H), 7.94 (d, 2H), 7.85 (d, 2H), 7.61

(t, 1H), 7.52–7.43 (m, 5H), 7.37 (d, 2H). FTIR (KBr, cm^{-1}): 480(s), 538(s), 562(m), 660 (m), 687(vs), 737(m), 775(w), 818(s), 915(m), 987(m), 1060(m), 1225(vs), 1321(m), 1407 (m), 1445(m), 1562(m), 1595(s), 1619(vs, C=N), 1674(vs, C=O), 2851(m), 3058(w), 3425 (wb). ESI MS: 314.3 (LH^+, 100%). UV–vis in CH_2Cl_2: λ, nm; (ε, M^{-1} cm^{-1}): 210 (16,500); 260 (24,200). Anal. Calcd for $C_{20}H_{15}N_3O$: C, 76.66; H, 4.82; N, 13.41. Found: C, 76.78; H, 4.79; N, 13.44%.

2.3. *Synthesis of [Zn(L)2Br2] (1)*

0.124 g (0.40 mM) of **L** was dissolved in 30 mL of acetonitrile to which 0.045 g (0.20 mM) of solid $ZnBr_2$ was added and the reaction mixture was stirred for 2 h. Yellow solid precipitate was filtered and dried in air. Needle-shaped transparent yellow, stable crystals suitable for X-ray analysis were obtained from chloroform solution of the yellow solid. Yield, 0.115 g (68%). FTIR (KBr, cm^{-1}): 438(m), 670(m), 756(s), 1215(vs), 1618(s, C=N), 1679(s, C=O), 3018(wb). Anal. Calcd for $C_{40}H_{30}N_6O_2ZnBr_2$: C, 56.39; H, 3.55; N, 9.87. Found: C, 56.44; H, 3.49; N, 9.92%.

2.4. *Synthesis of [Cd(L)2I2] (2)*

0.156 g (0.5 mM) of **L** was dissolved in 50 mL of acetonitrile to which 0.092 g (0.25 mM) of solid CdI_2 was added and stirred for 2 h. During stirring, crystalline yellow compound appeared was filtered, washed with 5 mL of acetonitrile, and dried in air. Yield, 0.148 g (60%). FTIR (KBr, cm^{-1}): 443(m), 672(m), 756(s), 1215(vs), 1624(s, C=N), 1680(s, C=O), 3018(wb). Anal. Calcd for $C_{40}H_{30}N_6O_2CdI_2$: C, 48.39; H, 3.05; N, 8.46. Found: C, 48.42; H, 3.07; N, 8.47%. Bright yellow single crystals were grown by direct diffusion of *n*-hexane into a dilute dichloromethane solution of the complex. It crystallizes with CH_2Cl_2.

2.5. *Synthesis of [Ag(L)2]ClO4 (3)*

N(4-pyridylmethylene)diphenylethanedione monohydrazone, **L** (0.190 g, 0.60 mM) was dissolved in 40 mL of methanol, to which 0.124 g (0.60 mM) of solid $AgClO_4$ was added and stirred for 2 h. During stirring no compound appeared. The yellow solution was kept in the refrigerator for 7 days. The light yellow compound precipitated was filtered off, washed with 5 mL of methanol, and dried in vacuum. Yield, 0.150 g (60%, with respect to metal). Yellow needle-like single crystals suitable for X-ray analysis were grown by direct diffusion of diethyl ether into a concentrated DMF solution of the complex. FTIR (KBr, cm^{-1}): 538 (m), 562(w), 620(m), 664(s), 690(s), 735(s), 770(s), 875(s), 910(w), 1090(vs, ClO_4^-), 1176 (m), 1225(s), 1361(m), 1440(s), 1560(s), 1599(vs, C=N), 1676(vs, C=O), 3540(wb). UV–vis in CH_2Cl_2: λ, nm; (ε, M^{-1} cm^{-1}): 215 (35,080); 267 (22,450). Anal. Calcd for $C_{40}H_{30}N_6O_6ClAg$: C, 57.60; H, 3.62; N, 10.08. Found: C, 57.67; H, 3.65; N, 10.14%.

2.6. *X-ray crystallography*

X-ray single crystal data were collected using MoKα (λ = 0.7107 Å) radiation on a BRUKER APEX II diffractometer equipped with a CCD area detector. Data collection, data reduction, structure solution/refinement were carried out using the software package of SMART APEX [34]. The structures were solved by direct methods (*SHELXS-97*) and

standard Fourier techniques, and refined on F^2 using full-matrix least-squares (*SHELXL-97*) using the *SHELX-97* package [35] incorporated in *WinGX* [36]. In most cases, non-hydrogen atoms were treated anisotropically. Whenever possible, hydrogens were located on a difference Fourier map and refined. In other cases, the hydrogens were geometrically fixed. The crystallographic details and refinement parameters of **1**, **2**·CH_2Cl_2, and **3** are summarized in table 1 and selected bond lengths and angles are listed in table 2.

2.7. *Assessment of antibacterial activity*

2.7.1. Test micro-organisms. Eleven bacterial cultures (eight Gram-negative; *Klebsiella pneumonia 114*, *Escherichia coli K88*, *Salmonella typhi ATCC 34*, *Pseudomonas aeruginosa ATCC 27853*, *Vibrio cholerae 14035*, *Salmonella typhimurium 11*, *Shigella dysenteriae 7*, and *Proteus vulgaris 21* and three Gram-positive; *Bacillus subtilis UC 564*, *Staphylococcus aureus ATCC25923*, and *Enterococcus faecalis*), and four fungal cultures (*Aspergillus niger*, *Aspergillus oryzae*, *Saccharomyces cerevisiae*, and *Penicillium notatum*) were used in this study of antimicrobial and antifungal activities of the compounds. All these organisms were collected from the Division of Microbiology, Department of Pharmaceutical Technology, Jadavpur University, Kolkata as a gift. The bacterial cultures were maintained in Nutrient Broth/Agar medium (Merck) at pH 7.2–7.4, whereas the fungal cultures were maintained in Czapek-Dox Broth/Agar medium (Merck) at pH 5.4 [37].

Table 1. Crystal data and refinement parameters of **1**, **2**·CH_2Cl_2, and **3**.

Compound	**1**	**2**·CH_2Cl_2	**3**
Formula	$C_{40}H_{30}N_6O_2ZnBr_2$	$C_{42}H_{36}N_6O_2Cl_2CdI_2$	$C_{40}H_{30}N_6O_6AgCl$
Formula weight	851.89	1093.94	834.02
Crystal system	Monoclinic	Monoclinic	Monoclinic
Space group	*C2/c* (No. 15)	*P2₁/m* (No. 11)	*P2₁* (No. 4)
a (Å)	25.343(3)	12.6146(8)	9.0889(16)
b (Å)	12.9201(11)	25.5940(18)	12.295(2)
c (Å)	12.4947(10)	13.2454(9)	33.502(6)
α (°)	90	90	90
β (°)	109.146(5)	90.128(2)	90.470(3)
γ (°)	90	90	90
V (Å^3)	3864.9(7)	4276.4(5)	3743.7(11)
Z	4	4	2
D (Calcd) (g/cm^3)	1.464	1.671	1.480
μ (Mo Kα) (mm)	2.745	2.117	0.666
F (0 0 0)	1712	2104	1696
Crystal size (mm)	0.18 × 0.12 × 0.05	0.20 × 0.14 × 0.12	0.20 × 0.15 × 0.12
Temperature (K)	293	293	293
Radiation (Å)	Mo K_α 0.71073	Mo K_α 0.71073	Mo K_α 0.71073
θ min–max (°)	1.8, 25.8	1.5, 30.0	0.6, 21.6
Data-set	$h=-29\rightarrow30$	$h=-16\rightarrow17$	$h=-9\rightarrow9$
	$k=-15\rightarrow15$	$k=-33\rightarrow33$	$k=-12\rightarrow2$
	$l=-15\rightarrow15$	$l=-18\rightarrow17$	$l=-34\rightarrow34$
Total data	23,373	49,791	26,329
Unique data	3734	11,901	8704
R(int)	0.056	0.045	0.049
Observed data [$I>2.0\sigma(I)$]	2345	6816	7375
N_{ref}	3734	11,901	8704
N_{par}	231	513	974
R	0.0358	0.0467	0.0351
wR_2	0.1399	0.1433	0.0841
S	0.90	1.03	1.04

Table 2. Selected bond distances (Å) and angles (°) in **1**, **2**·CH_2Cl_2, and **3**.

COMPOUND-**1**	*Bond distances*			
	Zn1–N4	2.067(3)	Zn1–Br2	2.3395(6)
	Bond angles			
	Br2–Zn1–N4	111.45(7)	N4–Zn1–$N4^i$	94.88(11)
	Br2–Zn1–$Br2^i$	120.44(3)	$Br2^i$–Zn1–$N4^i$	111.45(7)
	Br2–Zn1–$N4^i$	107.83(7)	Zn1–N4–C15	118.5(3)
	$Br2^i$–Zn1–N4	107.83(7)	Zn1–N4–C18	124.5(2)
	i = 1 − *x*, *y*, 3/2 − *z*			
COMPOUND-**2**·CH_2Cl_2	*Bond distances*			
	I1–Cd1	2.6861(8)	Cd1–$N1^i$	2.297(4)
	I2–Cd1	2.6961(8)	Cd1–N1	2.293(4)
	I3–Cd2	2.6908(6)	Cd2–$N4^i$	2.293(4)
	I4–Cd2	2.6914(6)	Cd2–N4	2.293(4)
	Bond angles			
	I1–Cd1–I2	109.01(7)	I3–Cd2–$N4^i$	107.10(7)
	I1–Cd1–N1	107.07(7)	I3–Cd2–I4	125.50(3)
	I1–Cd1–$N1^i$	107.06(7)	I3–Cd2–N4	107.10(7)
	I2–Cd1–N1	109.01(7)	N4–Cd2–$N4^i$	95.10(1)
	I2–Cd1–$N1^i$	109.01(7)	I4–Cd2–N4	108.96(7)
	N1–Cd1–$N1^i$	94.80(14)	I4–Cd2–$N4^i$	108.96(7)
	i = *x*, 3/2 − *y*, *z*			
COMPOUND-**3**	*Bond distances*			
	Ag1–O3	2.651(6)	Ag1–N1	2.136(5)
	Ag2–N7	2.135(5)	Ag2–N8	2.153(5)
	Ag1–N2	2.134(5)		
	Bond angles			
	O3–Ag1–N1	92.1(1)	O3–Ag1–N2	94.8(2)
	N7–Ag2–N8	171.8(2)	N1–Ag1–N2	172.0(2)

2.7.2. Antibacterial activity. The antibacterial activity was assessed by Agar diffusion method and then the minimum inhibitory concentration (MIC) was determined by the Broth dilution method [37–39]. For assessing the antibacterial activity of each compound, the solutions of the compounds were prepared in DMSO not exceeding 10% in the final solution. The diluents used for DMSO solution include sterile double distilled water. Standard antibiotics were streptomycin and tetracycline. The control used here contains only 10% DMSO and no growth inhibition was noted in the control.

In this method, fresh stock solutions of the compounds of 10 mg mL^{-1} were prepared which were further diluted with sterile distilled water. For screening of antibacterial activity by Agar dilution, the compounds of desired concentrations, 0 (control), 100, 200, 400, 600, 800, and 1000 μg mL^{-1}, were mixed with Mueller Hinton agar (MHA) and plated into sterile Petri dishes aseptically [40, 41]. One loop-full of bacterial suspensions previously grown in Nutrient Broth (2×10^6 cfu per spot) was inoculated on the MHA plates and was incubated at 37 °C for 18–24 h [41].

The inoculum suspension of the tested bacteria from the broth cultures was diluted in MHB to give a concentration of 1×10^6 cfu mL^{-1}. The compounds of desired concentrations were then added to each tube and were incubated at 37 °C (24 h). In each case, the test was performed in triplicate and the results were expressed as means. The MIC obtained was compared with two standard antibiotics streptomycin and tetracycline.

2.7.3. Antifungal activity. Antifungal activity was tested by the agar dilution method [38, 40]. The fungal strains were grown at 25–28 °C on Czapek-Dox broth for 48 h. The drugs mixed to Czapek-Dox agar to get a final concentration of 0 (control), 100, 200, 400, 600, 800, 1000, and 2000 μg mL^{-1} were plated into sterile Petri plates aseptically. One loop-full of fungal suspensions (2×10^5 spores mL^{-1}) was spotted on each plate and incubated at 28 °C for 48 h. The MIC was calculated by the Broth dilution method [41] with or without drugs of desired concentrations and a final concentration of fungal spores was taken as 1×10^5 spores mL^{-1} [40]. The tubes were incubated at 28 °C for 48 h. The results obtained were compared with a standard antifungal agent Nystatin.

3. Results and discussion

3.1. *Syntheses and characterizations of L, 1, 2, and 3*

Ligand **L** was synthesized by refluxing benzil monohydrazone and 4-pyridine carboxaldehyde in 1 : 1 M ratio in anhydrous methanol. It represents a spatially hindered molecule with enolimine and ketoamine tautomers. In the ^{1}H NMR spectra of **L**, the HC=N proton resonates at 8.52 ppm as a singlet, the pyridyl protons resonate as doublets at 8.60 ppm and 7.94 ppm. The other peaks in the ^{1}H NMR spectra of **L** are assigned as the phenyl protons. The FT-IR spectrum of **L** shows characteristic bands at 1674 and 1619 cm^{-1} which we assign to the C=O and imine C=N stretching frequencies, respectively. The absorption spectra of **L** (in dichloromethane) shows intraligand charge transfer bands at 260 nm (ε, 24,200 M^{-1} cm^{-1}) and 210 nm (ε, 16,500 M^{-1} cm^{-1}), respectively.

The Zn(II), Cd(II), and Ag(I) complexes, **1**, **2**, and **3**, were synthesized by simple reaction of $ZnBr_2$, CdI_2, and $AgClO_4$ with **L**, respectively, at room temperature in good yield (scheme 1). The complexes were only soluble in DMF and DMSO. Their solutions are quite stable in air. In **1**, **2**, and **3**, the IR stretching frequencies of C=O and C=N are at 1679, 1618 cm^{-1}; 1680, 1624 cm^{-1}; and 1676, 1599 cm^{-1}, respectively. In the electronic absorption spectra of **1**, **2**, and **3**, the π–π* transitions of the phenyl rings and pyridyl groups shift in comparison to the ligand.

3.2. *Description of the crystal structures of 1, 2·CH2Cl2, and 3*

X-ray crystallographic analyses reveal that **1** and **2** consist of mononuclear units where tetrahedrally coordinated metal ions (Zn(II) for **1** and Cd(II) for **2**) bind two ligands through

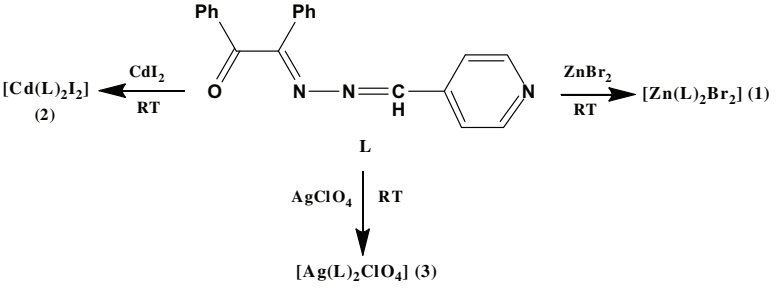

Scheme 1. Syntheses of the Zn(II)(**1**), Cd(II)(**2**), and Ag(I)(**3**) complexes of **L**.

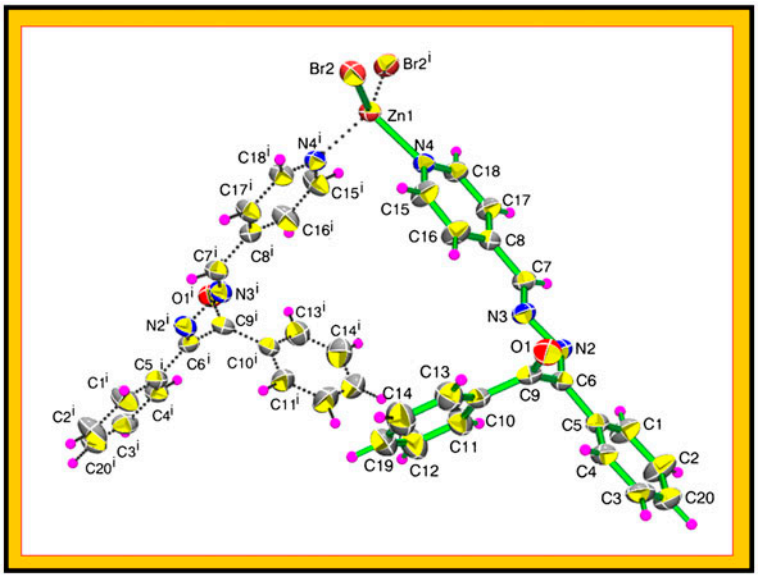

Figure 1. The ORTEP diagram (30% ellipsoidal probability) of **1** with atom numbering scheme (i = $1-x$, y, $3/2-z$; dotted part is the symmetric counterpart of the labeled part).

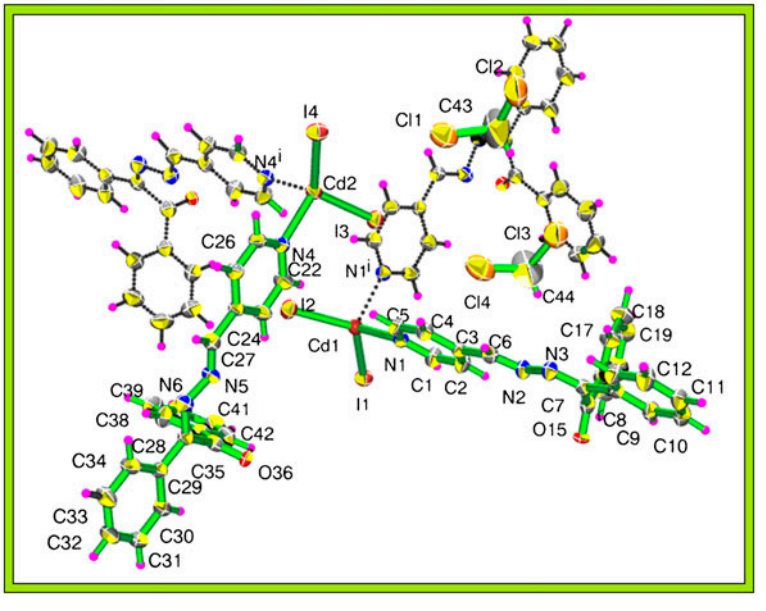

Figure 2. ORTEP diagram of **2·CH_2Cl_2** (30% ellipsoidal probability) with atom numbering scheme. Two solvent CH_2Cl_2 molecules are present in the asymmetric unit (i = x, $3/2-y$, z; dotted part is the symmetric counterpart of the labeled part).

the pyridine (figures 1 and 2). Two bromides and two iodides satisfy the other two coordination sites of tetrahedral Zn(II) and Cd(II), respectively. The coordination tetrahedra are slightly distorted. In **1**, Zn1–N4 distance is 2.067(3) Å, smaller than the Zn1–Br2 distance of 2.3395(6) Å (table 2). Similarly, the N4–Zn1–N4* (* = i = $1-x$, y, $3/2-z$) coordination angle of 94.88(11)° is the lowest and the Br-Zn-Br* coordination angle 120.44(3)° is the highest. N4–Zn1–Br* coordination angle is 107.83(7)°. The differences in bond distance and bond angle values clearly indicate the distorted Zn1 coordination environment.

There exist two different Cd centers (Cd1 and Cd2) in **2**, both having slightly distorted tetrahedral coordination. The Cd–I distances are 2.6861(8)–2.6961(8) Å (table 2) and all Cd–N distances are 2.297(4) Å. Two Cd centers possess nearly identical coordination angle ranges of 94.80(14)° [N–Cd–N] to 125.50(3)° [I–Cd–I angle]. This type of distortion in Zn (II) and Cd(II) coordination polyhedral is rather common [42, 43].

In **3**, Ag(I) coordinates linearly to two ligands (figure 3). The asymmetric unit of **1** consists of a single unit, whereas those of **2** and **3** consist of two independent units each, similar to previously reported coordination compounds [44, 45]. Coordination geometries of two independent Cd(II) units in **2** are the same, but for the two Ag(I) units in **3**, one Ag(I) is two-coordinate, and the other one is three-coordinate. Third coordination of Ag(I) in **3** is satisfied by oxygen of a perchlorate. Another perchlorate is also present in the asymmetric unit of **3**, but remains non-coordinated. The Ag–N distances are 2.134(5)–2.153(5) Å (table 2). The N1–Ag1–N2 angle is 172.0(2)° and N7–Ag2–N8 angle is 171.8(2)°. Two non-coordinated dichloromethane molecules are also present in the asymmetric unit of **2·CH_2Cl_2**. In **1**, **2**, and **3**, only the pyridyl nitrogen of the ligand coordinates, the inner azine and imine nitrogens as well as the peripheral carbonyl oxygen do not take part in metal coordination. In **1**, **2**, and **3**, the imine bond lengths are 1.260, 1.269, and 1.244 Å, respectively. The delocalization of the imine bond is not prominent in **1**, **2**, and **3**. The crystal structure of **L** is not reported.

Crystallographic data and refinement parameters for **1**, **2·CH_2Cl_2**, and **3** are given in table 1. Metal ligand coordination bond distances and angles for the coordination

Table 3. Hydrogen bond interactions in **1**, **2·CH_2Cl_2**, and **3** (Å, °).

D–H···A	D–H (Å)	H–A (Å)	D–A (Å)	⟨D–H···A (°)	Symmetry
Hydrogen bond interaction in **1**					
C15–H15···Br2	0.93	2.84	3.639(5)	145	$1-x$, $2-y$, $2-z$
Cl···π interaction in **2·CH_2Cl_2**					
Y–X···Cg(π-Ring)	X···Cg	X-Perp	Y–X···Cg	Y···Cg	
C43–Cl2···R4	3.603(3)	3.507	126.2(3)	4.820(2)	
C44–Cl4···R1	3.605(3)	3.506	126.1(3)	4.827(2)	
Hydrogen bond interaction in **3**					
D–H···A	D–H (Å)	H–A (Å)	D–A (Å)	<D–H···A (°)	Symmetry
C5–H5···O1	0.93	2.56	3.419(8)	154	$1+x$, y, z
C20–H20···O1	0.93	2.59	3.234(8)	127	$2+x$, y, z
C33–H33···O5	0.93	2.47	3.303(8)	149	$-1+x$, $1+y$, z
C21–H21···O6	0.93	2.55	3.428(10)	157	–
C46–H46···O6	0.93	2.44	3.168(9)	135	$1-x$, $1/2+$y, $1-z$
C31–H31···O11	0.93	2.54	3.365(9)	148	$-2+x$, y, z
C45–H45···O11	0.93	2.38	3.160(9)	142	$1-x$, $-1/2+y$, $1-z$
Cl–O···π interaction in **3**					
Y–X–Cg(i)	X–Cg(j) (Å)	X-perp (Å)	Y···Cg (Å)	Y–X···Cg (Å)	
Cl1–O5···R6	3.937(8)	3.417	4.665(3)	114.2(4)	$1+z$, $-1+y$, z
R6 → C35−C36−C37−C38−C39−C40					

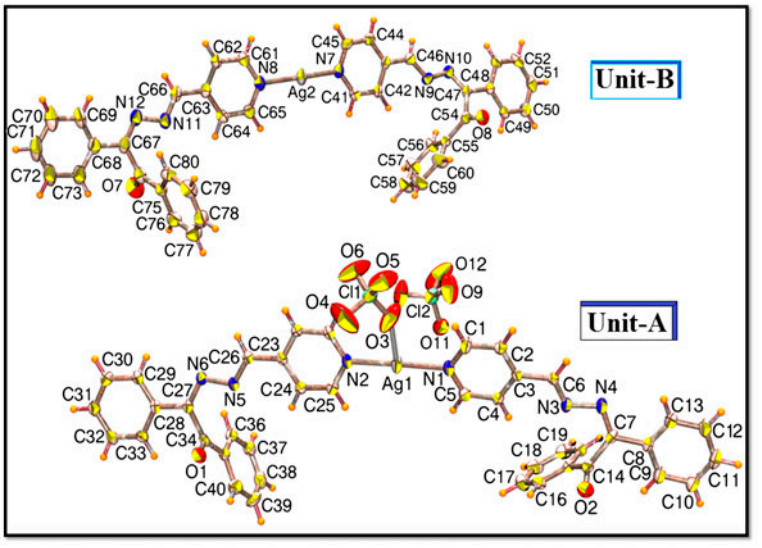

Figure 3. ORTEP diagram (30% ellipsoidal probability) with atom numbering scheme for **3**.

compounds are summarized in table 2. Coordination units of all the coordination compounds are normal.

Mononuclear units in **1** are assembled into a 1-D chain-like arrangement along the crystallographic *c*-axis through CH···Br interactions (table 3, figure S1, see online supplemental material at http://dx.doi.org/10.1080/00958972.2014.951346). A cyclic $R_2^2(9)$ [46] hydrogen-bonded motif is formed where the coordinated bromide of one unit is an acceptor

Table 4. π···π interaction data for **1**, **2**·$\mathbf{CH_2Cl_2}$, and **3**.

Ri···Rj	Symmetry	d_{cc} (Å)	α (°)	β (°)	d_{cv} (Å)
Complex **1**					
R1···R2	$2-x, 2-y, 1-z$	3.782(3)	8.70	23.17	3.628
R1 → N4–C15–C16–C8–C17–C18; **R2** → C1–C2–C20–C3–C4–C5					
d_{cc} = Centroid–centroid distance between ring i and ring j					
d_{cv} = Vertical distance from ring centroid i to ring plane j					
α = Dihedral angle between the first ring mean plane and the second ring mean plane of the partner molecule					
β = Angle between centroids of first ring and second ring mean planes					
Compound **2**·$\mathbf{CH_2Cl_2}$					
R1···R2	$1-x, 1-y, 1-z$	3.720(3)	4.1(3)	18.09	3.536(2)
R4···R5	$-x, 1-y, 2-z$	3.713(3)	3.9(3)	18.02	3.531(2)
R1 → N1–C1–C2–C3–C4–C5; **R2** → C8–C9–C10–C11–C12–C13; **R4** → N4–C22–C23–C24–C25–C26; **R5** → C29–C30–C31–C32–C33–C34					
Compound **3**					
R1···R2	$1+x, y, x$	3.858(3)	13.6(3)	24.07	3.642(2)
R2···R5	$1+x, y, z$	3.913(4)	10.3(3)	33.11	3.607(2)
R7···R8	$1+x, y, z$	3.765(4)	8.4(3)	18.41	3.440(2)
R7···R9	$-1+z, y, z$	3.772(4)	4.4(3)	23.15	3.553(3)
R8···R11	$1+x, y, z$	3.714(4)	7.5(4)	25.33	3.516(3)
R1 → N1−C1−C2−C3−C4−C5; **R2** → N2−C21−C22−C23−C24−C25; R3 → C8−C9−C10−C11−C12−C13; R5 → C28−C29−C30−C31−C32−C33; R7 → N7−C41−C42−C43−C44−C45; R8 → N8−C61−C62−C63−C64−C65; R9 → C48−C49−C50−C51−C52−C53; R11 → C68−C69−C70−C71−C72−C73					

Table 5. Determination of MIC of antibacterial activity.

Name of organism	MIC value μg mL^{-1} **L**	MIC value μg mL^{-1} **1**	MIC value μg mL^{-1} **2**	MIC value μg mL^{-1} **3**	MIC value μg mL^{-1} $ZnBr_2$	MIC value μg mL^{-1} CdI_2	MIC value μg mL^{-1} $AgClO_4$	MIC value μg mL^{-1} Strepto-mycin	MIC value μg mL^{-1} Tetracycline	10% DMSO
Bacillus subtilis UC564	_	400	500	450	750	100	150	0.8	1	_
Staphylococcus aureus ATCC25923	_	900	75	200	100	80	50	1	0.8	_
Klebsiella pneumoniae 114	700	500	40	100	100	75	100	0.9	1	_
Escherichia coli K88	850	475	45	300	50	80	80	0.8	0.5	_
S. typhi ATCC 34	900	950	100	150	200	75	50	5	0.8	_
P. aeruginosa ATCC27853	_	_	200	_	300	100	100	0.7	3	_
Vibrio cholerae 14035	_	40	50	100	200	35	50	6	0.8	_
Salmonella typhimurium 11	_	_	50	200	75	40	50	0.4	0.7	_
Enterococcus faecalis	_	_	200	200	_	100	100	0.7	0.8	_
Shigella dysenteriae 7	_	_	45	100	_	30	50	0.9	0.7	_
Proteus vulgaris 21	_	_	150	100	300	30	100	0.8	1	_

Note: – indicates no inhibition.

Table 6. Determination of Minimum Inhibitory Concentration (MIC) of antifungal activity.

Name of organism	MIC value (μg mL^{-1}) **L**	MIC value (μg mL^{-1}) **1**	MIC value (μg mL^{-1}) **2·CH_2Cl_2**	MIC value (μg mL^{-1}) **3**	MIC value (μg mL^{-1}) $ZnBr_2$	MIC value (μg mL^{-1}) CdI_2	MIC value (μg mL^{-1}) $AgClO_4$	MIC value (μg mL^{-1}) Nystatin
Aspergillus niger	>1000	>1000	750	>1000	>1000	>1000	>1000	4
Aspergillus oryzae	>1000	>1000	400	>1000	>1000	350	>1000	8
Penicillium notatum	500	1000	350	600	>1000	250	150	100
Saccharomyces cerevisiae	>1000	>1000	>1000	>1000	>1000	800	200	8

for the –CH donor of the pyridine group of the adjacent unit; π···π interactions between the terminal phenyl rings and the coordinated pyridine rings (table 4, figure S1) further unite these chains in three dimensions.

In **2**, the π···π interactions (table 4) between adjacent units are responsible for self-organization of the individual units in the *ab*-plane (figure S2). The dichloromethane molecules fill up the void region of the "V"-shaped units by Cl···π interaction (table 3). In **3**, molecular-complex units are arranged in successive layers; π···π (table 4), Cl–O···π (table 3), and Ag···O interactions come into play in the intermolecular interactions (figure S3). Weak C–H···O interactions (table 3) are also present along with the above-mentioned interactions in **3**.

3.3. *Antibacterial activity of L, 1, 2, and 3*

The results presented in table 5 show the antibacterial activities of **L**, **1**, **2**, and **3**. The results revealed that some of the species are not sensitive to the highest concentration tested here. The MIC values for 11 bacteria tested showed wide variation for **1**, **2**, and **3** and were not significant compared to the standard antibiotics, tetracycline and streptomycin. Here, the MIC values obtained for the coordination compounds were compared with salts of zinc ($ZnBr_2$), cadmium (CdI_2), and silver ($AgClO_4$) and in most cases, **L** alone fails to show antibacterial activity but **1**, **2**, and **3** exhibit potential antibacterial activity. **L** shows noticeable inhibitory effect only for *K. pneumoniae 114*, *E. coli K88,* and *S. typhimurium 11* which cause biliary tract infection, diarrhea, and typhoid fever, respectively.

3.4. *Antifungal activity of L, 1, 2, and 3*

The results presented in table 6 reveal that *P. notatum* was inhibited at a concentration of 500 and 600 μg mL^{-1} of **L** and **3**. *A. niger*, *A. oryzae,* and *Penicillium notatum* were inhibited at 750, 400, and 350 μg mL^{-1} concentration of **2**.

4. Conclusion

We synthesized an N_3O ligand, **L**, and its Zn(II), Cd(II), and Ag(I) complexes, **1** and **2**, and **3**. Though **L** contains four different ligating atoms (N_3O), all four donors cannot bind to one metal at a time because of its planar geometry. In **1**, **2**, and **3**, **L** is monodentate to the metal ions. The coordination compounds were characterized using various spectroscopic techniques and by X-ray crystallographic analysis. The antibacterial and antifungal activities of these complexes were also assessed. The MIC values for the compounds clearly indicated that **1**, **2**, and **3** were different from that of the constituent ligand and metal salts, also supported by structural analysis and other physicochemical parameters. **1**, **2**, and **3** are fairly good antibacterial agents and show a broad spectrum of activity. However, all three complexes were responsive at a concentration within 50 μg mL^{-1} for *Vibrio cholera* which is interesting as an agent of antienterobacteriaceae. The antifungal activities of the compounds with respective MIC values indicated that **2** is as good as CdI_2 so the complex might have therapeutic potential if its toxicity is significantly diminished compared to CdI_2. Dinuclear Ag(I)–N-heterocyclic carbene complex [29] exhibited potential activity against human colon cancer (HCT 116) and breast cancer (MCF-7), whereas our mononuclear N-coordinated Ag

(I) complex shows antimicrobial activity against *Klebsiella pneumoniae 114*, *E. coli K88*, *S. typhi ATCC 34*, *B. subtilis UC564,* and *S. aureus ATCC25923*. Sumathi *et al.* [47] reported the antimicrobial activities of diketimine metal complexes; in our study, we have tested the antimicrobial and antitumor activities of monoketimine metal complexes. In their case, all the complexes showed higher activity than the free ligand, but in our case, free **L** and **1** exhibit comparable inhibitory effect for *S. typhimurium 11*. None of the compounds tested here could be considered as likely competitors for antibiotics. In general, the complexes have better activity in comparison to the ligands but almost similar activity as the simple metal salts (e.g. $ZnBr_2$, CdI_2, etc.), although they might be less toxic. The studied compounds are not very effective as antifungal agents.

Supplementary material

CCDC No. 958514, 1010160, and 1010161 contains the supplementary crystallographic data for **1**, **2**·$\mathbf{CH_2Cl_2}$, and **3**, respectively. These data can be obtained free of charge via http://www.ccdc.cam.ac.uk/conts/retrieving.html.

Acknowledgments

G.K.P. thanks the Department of Science and Technology and Department of Biotechnology, Government of India, New Delhi for financial support.

References

[1] H. Schiff. *Ann. Suppl.*, **3**, 343 (1864).
[2] R. Hernandez-Molina, A. Mederos. In *Comprehensive Coordination Chemistry*, J.A. McCleverty, T.J. Meyer (Eds), Vol. 1, 2nd Edn, p. 411, Elsevier, Amsterdam (2004).
[3] M. Andruh, F. Tuna, M.A. Cato. *Focus on Organometallic Chemistry Research*, Vol. 144, Nova Publishers, Hauppauge, NY (2005).
[4] P.G. Cozzi. *Chem. Soc. Rev.*, **33**, 410 (2004).
[5] S. Yamada. *Coord. Chem. Rev.*, **190–192**, 537 (1999).
[6] A.J. Atkins, D. Black, A.J. Blake, A. Marin-Bocerra, S. Parsons, L. Ruiz-Ramirez, M. Schroder. *Chem. Commun.*, 457 (1996).
[7] P. Jiang, Z. Guo. *Coord. Chem. Rev.*, **248**, 205 (2004).
[8] N. Dharmaraj, N.P. Viswanalhamurthi, K. Natarajan. *Transition Met. Chem.*, **26**, 105 (2001).
[9] M. Tumer, H. Koksal, M.K. Sener, S. Serin. *Transition Met. Chem.*, **24**, 414 (1999).
[10] J.W. Pyrz, A.L. Roe, L.J. Stern, L. Que Jr. *J. Am. Chem. Soc.*, **107**, 614 (1985).
[11] M.Tumer, B. Erdogan, H. Koksal, S. Serin. M.Y. Nutku. *Synth. React. Inorg. Met. Org. Chem.*, **28**, 529 (1998).
[12] M. Sakamoto, K. Maneski, H. Okawa. *Coord. Chem. Rev.*, **219–221**, 379 (2001).
[13] M. Wang, H. Zhu, K. Jin, D. Dai, L. Sun. *J. Catal.*, **220**, 392 (2003).
[14] A.S. Al-Shiri. *Spectrochim. Acta*, **60A**, 118 (2004).
[15] K.A. Siddiqui. *J. Coord. Chem.*, **66**, 2039 (2013).
[16] S. Das, S. Pal. *Inorg. Chim. Acta*, **363**, 3028 (2010).
[17] M. Wałęsa-Chorab, A. Gorczyński, M. Kubicki, Z. Hnatejko, V. Patroniak. *Polyhedron*, **31**, 51 (2012).
[18] X. Qiao, Z.Y. Ma, C.Z. Xie, F. Xue, Y.W. Zhang, J.Y. Xu, Z.Y. Qiang, J.S. Lou, G.J. Chen, S.P. Yan. *J. Inorg. Biochem.*, **105**, 728 (2011).
[19] M.J. Hendrick, M.T. May, M.J. Plishka, K.D. Robinson. *Metals in Biological Systems*, Ellis Horwood, Chichester (1992).
[20] D.C. Ress, M. Lewis, W.N. Lipscomb. *J. Mol. Biol.*, **168**, 367 (1983).
[21] D.N. Silverman, S. Lindskog. *Acc. Chem. Res.*, **21**, 30 (1988).

[22] E.E. Kim, H.W. Wyckoff. *J. Mol. Biol.*, **218**, 449 (1991).
[23] P.A. Ochoa, M.I. Rodriguez-Tapiador, S.S. Alexandre, C. Pastor, F. Zamora. *J. Inorg. Biochem.*, **99**, 1540 (2005).
[24] (a) N.S. Oxtoby, N.R. Champness. *CrystEngComm*, **7**, 284 (2005); (b) E.-Q. Gao, A.-L. Cheng, Y.-X. Xu, C.-H. Yan, M.-H. He. *Cryst. Growth Des.*, **5**, 1005 (2005).
[25] E. Lõpez-Torres, M.A. Mendiola, C.J. Pastor. *Polyhedron*, **25**, 1464 (2006).
[26] (a) J.J.M. Amoore, C.A. Black, L.R. Hanton. *Cryst. Growth Des.*, **5**, 1255 (2005); (b) X.-C. Huang, J.-P. Zhang, Y.-Y. Lin, X.-M. Chen. *Chem. Commun.*, 2232 (2005).
[27] A. Brydson. *Rubbery Materials and Their Compounds*, Elsevier, London (1988).
[28] I.R. McDougall. *Thyroid Disease in Clinical Practice*, Chapman & Hall, London (1992).
[29] R.A. Haque, S.F. Nasri, M.A. Iqbal. *J. Coord. Chem.*, **66**, 2679 (2013).
[30] T.H. Noh, J.W. Lee, Y.-A. Lee, J.E. Lee, S.S. Lee, O.-S. Jung. *Bull. Korean Chem. Soc.*, **29**, 562 (2008).
[31] L.J. Parker, L.C. Italiano, C.J. Morton, N.C. Hancock, D.B. Ascher, J.B. Aitken, H.H. Harris, P. Campomanes, U. Rothlisberger, A. DeLuca, M. Lo Bello, W.H. Ang, P.J. Dyson, M.W. Parker. *Chem. Eur. J.*, **17**, 7806 (2011).
[32] W. Liu, R. Gust. *Chem. Soc. Rev.*, **42**, 755 (2013).
[33] D.H. Busch, J.C. Bailar. *J. Am. Chem. Soc.*, **78**, 1137 (1956).
[34] *SMART & SAINT Software Reference Manuals (Version 5.0)*, Bruker AXS Inc., 336, Madison, WI.
[35] G.M. Sheldrick. *Acta Crystallogr.*, **A64**, 112 (2008).
[36] L.J. Farrugia. *WinGX: An Integrated System of Windows Programs for the 339 Solution, Refinement and Analysis for Single Crystal X-ray Diffraction Data*, *340 Version 1.80.01*, p. 341, Department of Chemistry, University of Glasgow (2003); *Appl. Crystallogr.*, **32**, 837 (1999).
[37] R. Cruickshank, J.P. Duguid, B.P. Marmion, R.H.A. Swain. *Medical Microbiology*, p. 201, Churchill Livingstone, London (1989).
[38] D. Chattopadhyay, T. Mukherjee, P. Pal, B. Saha, R. Bhadra. *J. Antimicrob. Chemother.*, **42**, 83 (1998).
[39] E.W. Koneman, S.D. Allen, W.M. Janda, P.C. Schreckenberger, W.C. Winn Jr. *Color Atlas and Textbook of Diagnostic Microbiology*, 5th Edn, Lippincott, Philadelphia, PA (1997).
[40] A. Samanta, D. Chattopadhyay, C. Sinha, A.D. Jana, S. Ghosh, A. Mandal, A. Banerjee, O. Hendricks, J.B. Christensen, J.E. Kristiansen. *Anti-Infective Agents*, **10**, 95 (2012).
[41] B. Chakraborty, A. Samanta, P.K. Sharma, M.S. Chhetri, S. Kafley, A. Banerjee, C. Sinha. *J. Chem. Pharm. Res.*, **2**, 731 (2010).
[42] S.L. Xiao, Y.Q. Zhao, C.H. He, G.H. Cui. *J. Coord. Chem.*, **66**, 89 (2013).
[43] B. Liu, R. Wang, G. Jin, X. Meng. *Coord. Chem.*, **66**, 1784 (2013).
[44] J. Qu, Y.-L. Yi, Y.-M. Hu, W.-T. Chen, H.-L. Gao, J.-Z. Cui, B. Zhai. *J. Coord. Chem.*, **65**, 3740 (2012).
[45] R. Kruszynski, T. Sieranski, M. Swiatkowski, M. Zielak, J. Wojciechowski, M. Dzierzawska, B. Lewinski. *J. Coord. Chem.*, **67**, 1332 (2014).
[46] M.C. Etter, J.C. MacDonald, J. Bernstein. *Acta Crystallogr.*, **B46**, 256 (1990).
[47] S. Sumathi, P. Tharmaraj, C.D. Sheela, R. Ebenezer. *J. Coord. Chem.*, **65**, 506 (2012).